# Determination of Equivalent Axle Load Factors with the use of strain energy of distortion

Dawid Ryś[a]* and Francesco Canestrari[b]

[a] *Faculty of Civil and Environmental Engineering, Gdansk University of Technology –*
*Gdansk  – Poland; dawrys@pg.edu.pl*
[b]*Università Politecnica delle Marche – 60131 Ancona – Italy; f.canestrari@staff.univpm.it*

*\* corresponding author*

1

# Determination of Equivalent Axle Load Factors with the use of strain energy of distortion

This paper proposes a new method for calculation of equivalent axle load factors based on the analysis of strain energy of distortion induced in road pavements by traffic loads. The relationship between the rate of change of the averaged released pseudostrain energy and fatigue life of asphalt mixture is included in the new method as well. The main advantage of the method is the more accurate calculation (i.e. closer to the real behaviour observed in field) of the effects of multiple axles and super single tyres versus dual tyres. The proposed approach also enables consideration of the location of critical points, at which strain energy of distortion reaches extreme values. In most cases maximum energy of distortion is observed at the bottom of asphalt layers. Nevertheless, it was noted that in the case of thick structures loaded by heavy axles, maximum values are observed at the top of asphalt layers. When single axles are considered, the function of equivalent axle load factor takes on the form of the well-known power equation with the exponent ranging from 2.7 to 5.3. It was proved in the paper that the damaging effect of triple axles on asphalt pavement is several times higher than the damaging effect of three single axles carrying the same load, but at a greater distance to each other. Due to this fact, traffic load may be significantly underestimated in many pavement design methods. Consequently, this may explain why the actual service life of road pavements is often lower than the predicted design value.

**Keywords:** Load Equivalency Factors, Equivalent Standard Axle Load, Strain Energy, fatigue life, asphalt pavement, fatigue cracking

## Introduction

Equivalent axle load factors (EALF) are used to determine the relative damaging effect of real traffic on road pavements. Based on EALF, the design traffic is calculated, serving as the main input for pavement structure design and determination of the requirements for road materials. Historically, the concept of EALF was introduced after the AASHO road test in 1960. The original equations developed on the basis of empirical observations were further simplified into the "fourth power equation". According to later works, the exponent $n$ in the power equation can range from 2 (COST 334, 2001) to 5 (*French Design Manual for Pavement Structures,*

2

*Guide technique*, 1997) for asphalt pavements and from 4 to 20 for semi-rigid and rigid pavements ( Judycki, 2010, 2011). Judycki (2010, 2011) also proved that the exponent *n* depends on the fatigue criteria used for pavement design. Power equation is widely used to convert the real number of vehicles into the number of equivalent standard axle loads, despite its empirical origin. Examples of use of the power equation with exponent 4 to calculate traffic loads include the design methods used in the UK (Atkinson, Merrill, & Thom, 2005), Germany (Sieber, 2012) and Poland (D. Rys, Judycki, & Jaskula, 2016).

Mechanistic-Empirical Pavement Design Guide M-EPDG (ARA Inc., 2004) is a design method which omits the conversion of traffic into the number of equivalent standard axles. According to M-EPDG, each pass of vehicle is transformed into damage and cumulative damage is further transformed into distress. The method considers different types of pavement distress separately, and in the case of flexible pavements the distresses are divided into fatigue cracking (taking into account bottom-up and top-down schemes), rutting and thermal cracking (which does not result from traffic). Determination of resilient strain at critical points under axle load is a crucial element in the process of damage calculation. The single maximum value of strain is chosen as representative and then inserted into the fatigue formula. However, the state of stresses and strains in front of and behind the centre of the axle is completely omitted. The single strain value may not be fully representative by itself, especially when dual tyres versus super single tyres and multiple axles versus single axles are considered.

This paper presents a new method for determination of equivalent axle load factors. According to this method, pavement response under wheel load is expressed by the total strain energy of distortion introduced into the pavement by a single pass of a wheel or a group of wheels. Such a concept enables inclusion of the entire complex course of changes in stresses and strains in pavement during the passage of wheel and expresses the corresponding global effect with one parameter. The subsequent calculation of the EALFs was based on the number

of wheel loads resulting in failure of asphalt mixture, determined using the dissipated energy theory, which has also recently been adopted in the design methods involving linear viscoelastic continuum damage of asphalt mixtures (Braham & Underwood, 2016; Sabouri & Kim, 2014; Zhang, Sabouri, Guddati, & Kim, 2013).

**Theoretical explanation**

*Strain energy introduced by a moving wheel*

A resilient and layered model of pavement structure is considered. As a consequence of a wheel load applied to the pavement structure, potential energy is generated in the pavement body. According to Huber (1904), the material effort can be measured by specific strain energy. When this approach is applied to an elastic pavement model, the elastic strain energy per unit volume is expressed as follows:

$$u_t = \frac{1}{2}(\sigma_1\varepsilon_1 + \sigma_2\varepsilon_2 + \sigma_3\varepsilon_3) = \frac{1}{2E}\left(\sigma_1^2 + \sigma_2^2 + \sigma_3^2 - 2v(\sigma_1\sigma_2 + \sigma_2\sigma_3 + \sigma_1\sigma_3)\right) \qquad (1)$$

Where:

$u_t$: strain energy [J/m$^3$],

$\sigma_1$, $\sigma_2$, $\sigma_3$: principal stresses [Pa],

$\varepsilon_1$, $\varepsilon_2$, $\varepsilon_3$: principal strains [-],

E: elastic modulus [Pa],

$v$: Poisson's ratio [-].

According to equation (2), strain energy consists of two components: the strain energy responsible for the change of volume $u_v$ and the strain energy of distortion $u_s$ responsible for the change of shape.

$$u_t = u_v + u_s \qquad (2)$$

Strain energy of distortion can be calculated according to the following formula:

$$u_s = \left(\frac{1+v}{6E}\right)[(\sigma_1 - \sigma_2)^2 + (\sigma_2 - \sigma_3)^2 + (\sigma_3 - \sigma_1)^2] \qquad (3)$$

4

The hypothesis posed by (von Mises, 1913) is that change in material shape is a possible source of its failure. Thus, strain energy of distortion expresses the response directly related to the damaging effect of a load applied to a pavement structure. In further works of (D. Beer, Fisher, & Jooste, 1997; Perdomo & Nokes, 1993) it was indicated that locations in pavement structure with relatively higher values of strain energy of distortion (so-called "hot spots") will potentially fail first – before locations with lower values. In a transverse section of a loaded pavement, strain energy concentrates in some areas. Due to the observed typical phenomena of fatigue crack evolution, it is expected that the critical point at the bottom of the asphalt layers as well as the critical points at the edge of tyre on the top surface will be subjected to the highest values of strain energy of distortion.

When a wheel passes over a given point, strain energy induced both in front of the wheel (i.e. before its passage) and behind it (i.e. after its passage) also contributes to evolution of damage at this point. Thus, strain energy of distortion induced by a single passage of wheel can be calculated according to the formula:

$$U_d = \int u_s(x)dx \tag{4}$$

where

$U_d$: strain energy of distortion induced at a given point by the moving wheel load [J/m$^2$],

$x$: distance along the direction of the moving wheel load [m].

### Relationship between strain energy of distortion and fatigue life of asphalt mixtures

In case of a perfectly resilient material, strain energy is fully recovered after unloading. Because of the elasto-visco-plastic nature of asphalt mixture, some portion of energy is dissipated in each load cycle. Dissipated energy is distributed into 1) visco-elastic damping and 2) incremental damage, resulting in permanent deformation and cracking formation. Some authors (van Dijk, 1975; van Dijk & Visser, 1977) initially presented an idea to quantify the energy consumed during fatigue damage accumulation and relate it to the final fatigue damage.

5

However, such studies did not solve the problem of appropriate separation of the dissipated energy into individual components. Other authors (Ghuzlan & Carpenter, 2000) assumed that the energy from viscoelastic damping within the dissipated strain energy at each cycle does not change significantly during the loading history. Based on this assumption, a concept of the ratio of change in dissipated energy between two cycles (RDEC) was developed. More recent studies (Shen, Airey, Carpenter, & Huang, 2006; Shen & Carpenter, 2007) indicated that in a certain range of load cycles RDEC takes a stable value, and authors designated it as the plate value PV. They also found a strong correlation between PV and the number of cycles till reduction of stiffness to 50% of its initial value ($N_f50$). Further research indicated that PV depends on the mode of loading (Bhasin, Castelo Branco, Masad, & Little, 2009). In studies of (Zhang et al., 2013) and (Sabouri & Kim, 2014) the $G^R$ method, which includes the mode of loading, was developed. The $G^R$ parameter characterizes the overall rate of damage accumulation during fatigue testing. Formula (5) was proposed by (Sabouri & Kim, 2014):

$$G^R = \frac{\overline{W_C^R}}{N_f} = \frac{\int_0^{N_f} W_C^R}{N_f^2} \tag{5}$$

where: $G^R$ is the rate of change of the averaged released pseudostrain energy (per cycle) throughout the entire history of the test, whereas $W_C^R$ is the total released pseudostrain energy per load cycle [J/m³]. Higher values of $G^R$ mean higher capacity for energy dissipation before failure. $W_C^R$ is considered as a comprehensive energy measure that quantifies dissipated energy under the action of external loading and includes material fatigue properties. It is reasonable to hypothesize that $\overline{W_C^R}$ is proportional to strain energy of distortion $U_d$ (see equation (4)):

$$\overline{W_C^R} = \beta U_d \tag{6}$$

where $\beta$ is an unknown coefficient of proportion between strain energy of distortion $U_d$ (4) and the total dissipated energy $\overline{W_C^R}$. Both $U_d$ and $\overline{W_C^R}$ are released with the use of the same wheel load. The difference is that $U_d$ is a parameter calculated on the basis of a resilient model

6

of pavement structure, whereas $\overline{W_C^R}$ quantifies the dissipated energy which causes fatigue damage in asphalt mixture.

In the studies of (Sabouri & Kim, 2014) the relationship between $G^R$ and fatigue life $N_f$ were found as the fundamental property of a given asphalt mixture.

$$G^R = A N_f^{\alpha} \tag{7}$$

Where:

A: model constant, takes on values ranging from $0.5 \cdot 10^8$ to $2 \cdot 10^8$,

α: model exponent (material coefficient), takes on values from $-1.505$ to $-1.375$.

After substituting equation (7) into equation (5), the following equation is obtained:

$$\overline{W_C^R} = A N_f^{\alpha+1} \tag{8}$$

Further substitution of formula (8) into equation (6) provides the theoretical relationship between strain energy of distortion and fatigue life of an asphalt mixture:

$$N_f = \left(\frac{\beta}{A} U_d\right)^{\frac{1}{\alpha+1}} \tag{9}$$

where:

$N_f$: fatigue life, number of wheel passes till pavement failure,

$U_d$: strain energy of distortion introduced into a given point by a passing wheel or a group of wheels,

$A$, $\alpha$: parameters reflecting the asphalt mixture fatigue performance, obtained on the basis of laboratory tests,

$\beta$: parameter relating strain energy of distortion in a theoretical resilient model to the total pseudostrain energy released during laboratory test. The parameter (or function) $\beta$ is unknown and it could be obtained on the basis of both full-scale field tests and laboratory tests.

### *Determination of equivalency axle load factor*

Pavement resistance under traffic loading is commonly expressed as the number of equivalent standard axle loads (ESALs) resulting in pavement failure. The exact moment of pavement failure depends on the assumed fatigue criteria; in the case of flexible pavements, fatigue cracking and permanent deformation criteria are predominantly considered. The following equation is valid for calculations of ESAL for both criteria:

$$ESAL = NV \cdot TF \tag{10}$$

where:

$NV$: total number of vehicles to pavement failure (also simply referred to as "traffic"),

$TF$: truck factor, which expresses the number of equivalent standard axle loads per one vehicle and can be calculated according to the equation (11):

$$TF = \sum_{i=1}^{4} LEF_i \cdot a_i \tag{11}$$

where:

LEF: load equivalency factor,

$a$: average number of axles per one vehicle,

$i$: type of axle (single, tandem, tridem, quad).

Load equivalency factor is calculated as the sum of multiplications of axle load spectrum (ALS) by the function of equivalent axle load factor across the entire range of axle loads. It is expressed by the following formula:

$$LEF = \sum_{j=1}^{l} F_j m_j \tag{12}$$

where:

$F_j$: equivalent axle load factor for axle load $Q_j$,

$m_j$: percentage of loads in the interval $j$ obtained from ALS,

8

$l$: total number of load intervals.

Equivalent axle load factor $F_j$ is defined as the ratio between the total number of passes to failure $N_{f,s}$ of the standard axle load $Q_s$ and the number of passes to failure $N_{f,j}$ of the actual axle load $Q_j$ for the same pavement structure:

$$F_j = \frac{N_{f,s}}{N_{f,j}} \tag{13}$$

When fatigue life is expressed by equation (9), equation (13) takes the following form:

$$F_j = \left(\frac{U_{d,s}}{U_{d,j}}\right)^{\frac{1}{\alpha+1}} \tag{14}$$

where:

$U_{d,s}$: total strain energy of distortion introduced by one pass of a wheel of the standard axle [J/m$^2$],

$U_{d,j}$: total strain energy of distortion introduced by a pass of a wheel (or wheels) of the actual axle,

$\alpha$: material coefficient (see equation (7)).

After substituting the values of parameter $\alpha$ (from -1.505 to -1.375), equation (14) becomes:

$$F_j = \left(\frac{U_{d,j}}{U_{d,s}}\right)^{n} \tag{15}$$

Where exponent $n$ takes on values in the range from 1.98 to 2.66 and, like coefficient $\alpha$, depends on the fatigue properties of the asphalt mixture. The ratio $U_{d,j}/U_{d,s}$ is unique for a given loading condition and pavement structure. Some cases are presented and discussed in the paper.. The analysis presented in further parts of the paper proves that the power relationships between ratios $U_{d,j}/U_{d,s}$ and $Q_j/Q_s$ do exist. Thus, formula (15) can be transformed to the form of the well-known power formula (16):

$$F_j = A \left(\frac{Q_j}{Q_s}\right)^{k} \tag{16}$$

9

Where:

$Q_j$ : actual axle load,

$Q_s$ : standard axle load,

$A$: factor related to axle or wheel type,

$k$ : exponent.

**Asphalt pavement structures**

For the analysis three significant types of asphalt pavement structure were assumed according to the Polish Catalogue of Typical Flexible and Semi-Rigid Pavements (General Directorate for National Roads and Highways, 2014; J. Judycki et al., 2017):

(1) KR1 A3 – representative of thin flexible structures for low traffic volume, with asphalt concrete used for both the wearing course and the asphalt base, with granular base made of natural aggregate.

(2) KR5 A1 – representative of flexible structures for moderate traffic, with stone matrix asphalt (SMA) used for the wearing course, asphalt concrete used in the binder and base courses, with unbound granular base of crushed stone.

(3) KR7 C – representative of thick semi-rigid structure for heavy traffic, with stone matrix asphalt (SMA) used for the wearing course, asphalt concrete used in the binder and asphalt base courses, with cement-treated C8/10 class base (according to the EN 14227-1 standard).

The mechanical properties (E, $v$) and thickness (H) of all pavement layers are summarized in Table 1. Stiffness modulus values of asphalt layers were assumed as for equivalent temperature 13°C, which is used for design of flexible pavements in Poland.

**Table 1.** Thickness and material properties of pavement layers

| layer | | Pavement structure properties | | | | | | | | |
| --- | --- | --- | --- | --- | --- | --- | --- | --- | --- | --- |
| | | KR1 A3 | | | KR5 A1 | | | KR7 C | | |
| no. | name | H [m] | E [MPa] | $\upsilon$ [-] | H [m] | E [MPa] | $\upsilon$ [-] | H [m] | E [MPa] | $\upsilon$ [-] |
| 1 | wearing course | 0.04 | 9270 | 0.3 | 0.04 | 7330 | 0.3 | 0.04 | 7330 | 0.3 |
| 2 | binder course | - | - | - | 0.08 | 10300 | 0.3 | 0.08 | 10300 | 0.3 |
| 3 | asphalt base | 0.05 | 8840 | 0.3 | 0.12 | 9820 | 0.3 | 0.12 | 9820 | 0.3 |
| 4 | unbound base | 0.25 | 250 | 0.3 | 0.20 | 400 | 0.3 | - | - | - |
| 5 | cement treated base | - | - | - | - | - | - | 0.24 | 3000 | 0.25 |
| 6 | subgrade | ∞ | 80 | 0.35 | ∞ | 120 | 0.35 | ∞ | 120 | 0.35 |

The standard 100 kN axle load was assumed according to the Polish catalogue. Since the standard axle is equipped with two single tyres, a 50 kN wheel load is applied by circular contact area with a constant inflation pressure of 850 kPa. The pavement models were loaded by single wheels with loads ranging from 20 kN to 60 kN, applied over a circular area with constant contact pressure equal to 850 kPa. Model KR5 A1 will be used as an example to describe the application of the method in detail. At the first stage, the pavement structure was loaded by single axles equipped with single tyres and with various loads. Subsequently, the effects of single and dual tyres used in an axle with standard load of 100 kN were considered. The model KR5 A1 was also loaded by three wheels moving at the distance of 1.3 m from each other in order to discuss the effect of triple axles. Finally, equivalent axle load factors were calculated for the remaining two models of pavement structure – thin flexible pavement KR1A3 for light traffic and thick semi-rigid pavement for extremely heavy traffic. All calculations were performed using the Bisar 3.0 software.

**Results and discussion**

*Distribution of strain energy of distortion in asphalt layers under single wheel with standard load*

Figure 1 presents the distribution of strain energy of distortion in a section transverse to the direction of traffic. The flexible pavement KR5 A1 was loaded with a single wheel, corresponding to the load of super single tyres. The applied load applied equalled 50 kN and the contact pressure equalled 850 kPa. This load is defined as the standard configuration used for design of flexible pavements in several European countries.
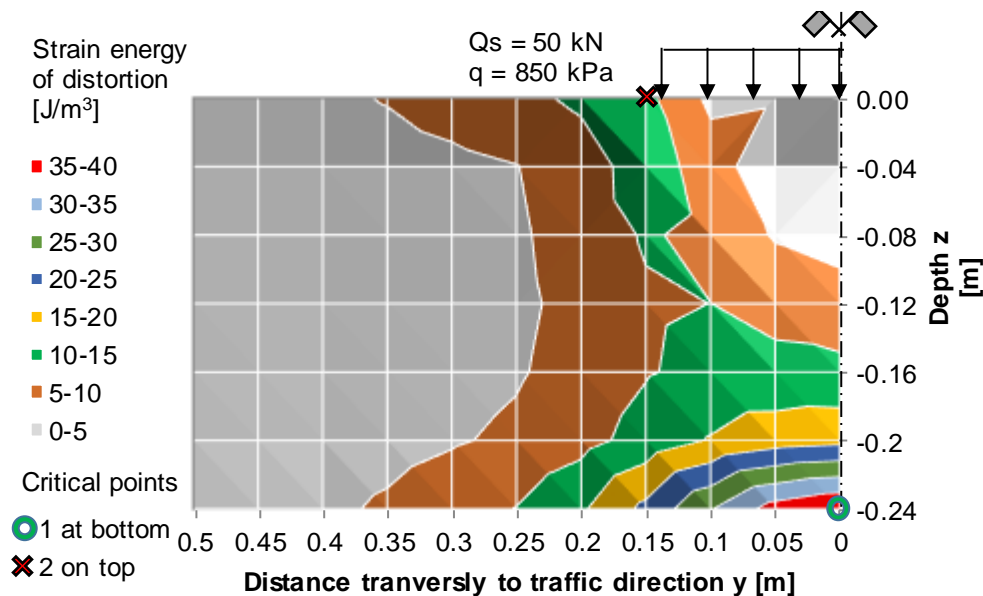


**Figure 1.** Distribution of strain energy of distortion in a transverse section of flexible pavement KR5 A1 for moderate traffic

It can be observed that two critical points with the local maximum density of strain energy of distortion occur for the case considered in Figure 1:

- Point 1 at the bottom of asphalt layer, directly below the centre of the circular load
- Point 2 on the top surface, at the edge of the circular load.

The presented locations of critical points are accurate for single wheels. Since dual wheels cause a different pavement reaction, the position of critical points is different, as will be discussed in greater detail in further parts of the paper. In the studies of (M. De Beer, Maina, Van Rensburg,

12

& Greben, 2012) detailed analyses of the critical points for various models of contact area were performed. It was established in these studies that when a non-uniform contact pressure model is considered, strain energy of distortion can be increased by a maximum factor of 2.8. Regardless of the type of wheel and models of contact area and contact pressure, critical points occur both at the bottom and at the top of asphalt layers, which is in agreement with the general observations of fatigue crack formation (Canestrari & Ingrassia, 2020) (Moreno-Navarro & Rubio-Gámez, 2016) (Mackiewicz, 2018) (Ingrassia, Spinelli, Paoloni & Canestrari, 2020).

The values of strain energy of distortion were also calculated longitudinally, along the direction of traffic movement. Calculations were limited to critical points which occur at the bottom of asphalt layers (under the centre of the load) and on the surface (at a transverse distance y = 15 cm, close to the edge of the wheel footprint).
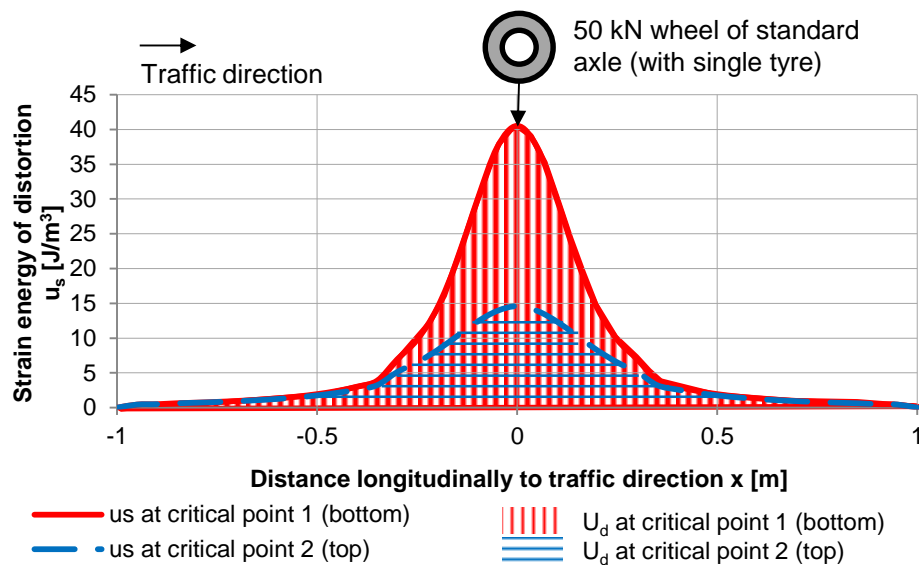


**Figure 2.** Strain energy of distortion $u_s$ at critical points vs. the distance from the centre of standard wheel load, longitudinally to traffic direction

The total strain energy of distortion induced by one pass of wheel $U_d$ (see equation (4)) can be expressed graphically at a given critical point as the area under the curve of $u_s$ in Figure 2. For the passage of the standard axle wheel load considered in Figure 2, the total strain energy

13

of distortion at critical point 1 (bottom of asphalt layers) equals

$U_{d,1} = 20.41 \ \frac{J}{m^2}$ and at critical point 2 (top surface) $U_{d,2} = 9.94 \ \frac{J}{m^2}$.

### *Total strain energy of distortion under single wheel with various loads*

Calculations performed for single wheels with loads ranging from 20 kN to 60 kN (corresponding to axles with single tyres and loads from 40 kN to 120 kN) are given in Figure 3. Two approaches to contact area and pressure were considered:

1) constant contact pressure equal to 850 kPa (Figure 3 a), where the radius of circular contact area varies from 9 cm for the wheel load of 20 kN to 15 cm for the wheel load of 60 kN;

2) constant circular contact area with radius equal to 15 cm, where the contact pressure varies from 280 kPa for the wheel load of 20 kN to 850 kPa for the wheel load of 60 kN.

The constant contact pressure approach is used commonly (i.a. in the Mechanistic-Empirical Pavement Design Guide), despite the fact that it is not the only approach to determination of pavement response under variable axle loads. Numerous studies may be found in the literature devoted to accurate description of the contact area and contact pressure, including the highly accurate non-uniform 3D tyre-pavement contact stress model (Hernandez, Gamez, Al-Qadi, & De Beer, 2014) or the linear model of contact area and contact stress, which is less accurate, but simpler in application (Hamlat, Hammoum, & Kerzreho, 2015).

14
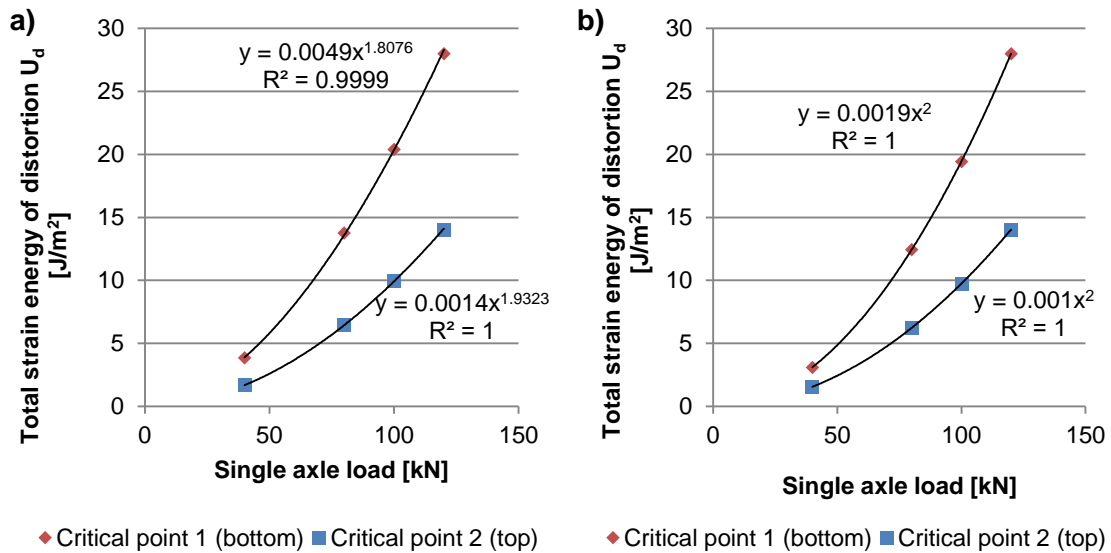
**Figure 3.** The total strain energy of distortion $U_d$ introduced at critical points 1 and 2 by axles equipped with single tyres and various loads for a) constant contact pressure 850 kPa and b) constant circular contact area with radius a = 15 cm

On the basis of the results showed in Figure 3 it can be expected that cracks will be initiated at the bottom of the asphalt layers, because strain energy of distortion for the standard axle load is two times greater at the critical point 1 than at the critical point 2. The exponent in the power relationship between $U_d$ and the axle load is equal to 2 both in the calculation performed with constant contact pressure and the calculation with constant circular area. Due to this fact, only the approach with constant contact pressure was considered in further analysis.

### *Equivalent axle load factors for single axles with super single tyres*

The ratio between the total strain energy of distortion introduced by actual axles vs. the standard axle $U_{d,j}/U_{d,s}$ is given in Figure 4a. In Figure 4b the range of equivalent standard axle load factor is also calculated according to Equation (14) and assuming that the material coefficient α takes on values in the range of −1.505 to −1.375. The exponent $k$ in power equation (16) obtained for a single axle takes on values from $k = 3.58$ for critical point 1 (bottom) and $n = 1.98$, to $k = 5.15$ for the critical point 2 (top) and $n = 2.67$. Parameter A remains constant and

15

equal to 1.0, regardless of the critical point. The relationships given in Figure 4b match the general 4th power rule when the case of single axles is considered and the same type of single wheels is assumed for all axles. In Figures 4a) and 4b) the x-axis presents a standardized form of axle load, expressed as the ratio between the actual axle load and the standard axle load. This form enables quick calculation of EALF for any level of standard load. The coefficient of determination $R^2$ is higher than 0.99 for every relationship.
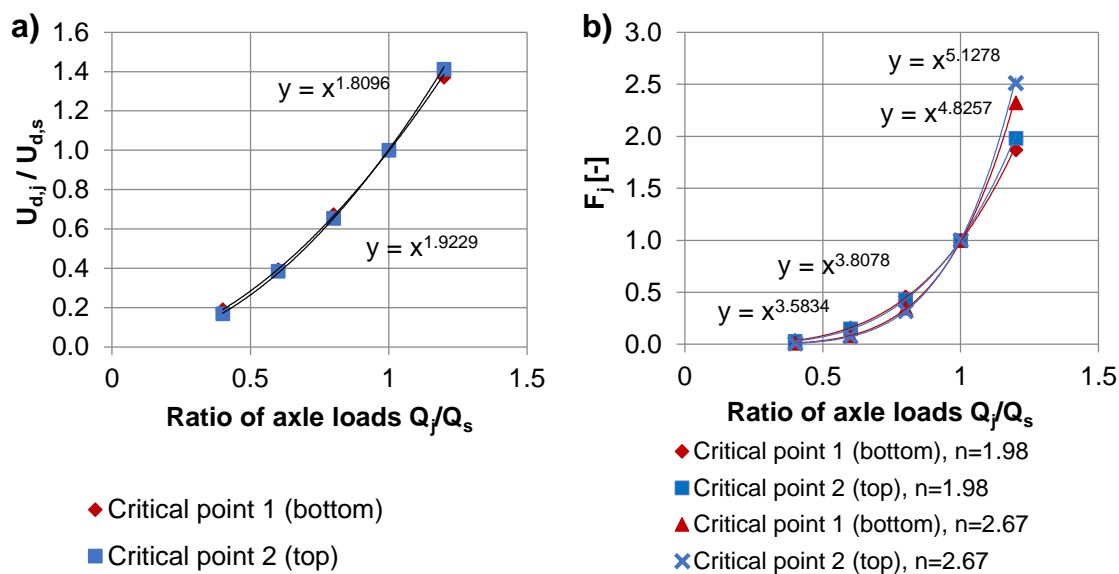


**Figure 4.** a) Ratio between the total strain energy of distortion introduced by a pass of actual single axle vs. standard axle $U_{d,j}/U_{d,s}$ b) equivalent axle load factor $F_j$ for single axles and single tyres, with exponent $n$ in Equation (15) equal to 1.98 or 2.66

*Comparison of equivalent axle load factors for super single and dual tyres*

       Pavement structure KR5 A1 was loaded by 100 kN axle equipped with dual tyres. Each tyre loads the pavement model with 25 kN and the contact pressure of 850 kPa. The distance between the centres of the two circular load areas was assumed as 35 cm. Transverse distribution of strain energy of distortion is different in the case of a single tyre (Figure 1) and a dual tyre (Figure 5), despite the same axle load (100 kN). The maximum strain energy of

16

distortion at the bottom of asphalt layers equals $u_s = 40$ J/m$^3$ in the case of single tyre, which is two times greater than in the case of dual tyre (compare Figure 1 to Figure 5). Another difference is that the critical point at the top of the asphalt layers is shifted. In the case of single tyre load, the critical point occurs at the edge of the load area, while in the case of dual tyres it occurs in the middle of the distance between tyres. The value of strain energy of distortion at the top of asphalt layers is similar in both cases and equals $u_s = 14$ J/m$^3$.

The values of the total strain energy of distortion as well as the equivalent axle load factors for super single and dual tires were calculated and compared in Table 2.
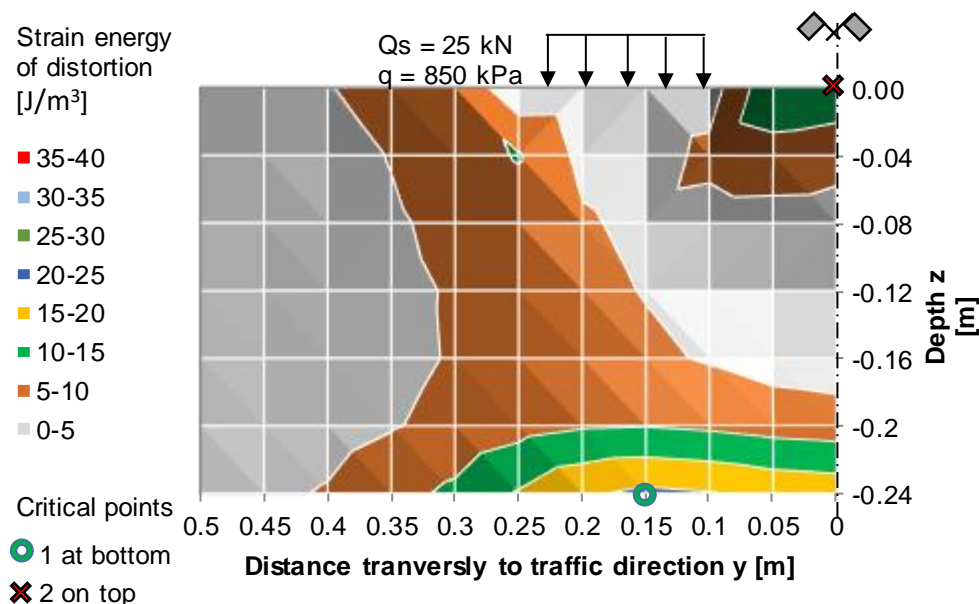


**Figure 5.** Distribution of strain energy of distortion in a transverse section of flexible pavement KR5 A1 in the case of application of dual axle

**Table 2.** Comparison of $U_d$ and ESAL of axles equipped with super single tyres and dual tyres

| Critical point: | | 1 (at the bottom of asphalt layers) | 2 (at the top of asphalt layers) |
|---|---|---|---|
| Total strain energy of distortion | Standard axle equipped with super single tyres $U_{d,single}$ [J/m$^2$] | 20.41 | 9.94 |
| | Standard axle equipped with dual tyres $U_{d,dual}$ [J/m$^2$] | 9.70 | 7.62 |
| Ratio of strain energy of distortion $U_{d,dual}$ / $U_{d,single}$ | | 0.48 | 0.77 |
| Equivalent axle load factor $F_j$ for material coefficient α: | α = −1.505 | 0.23 | 0.59 |
| | α = −1.375 | 0.14 | 0.49 |

From Table 2 it can be concluded that EALF for bottom-up cracks decreases from 1 to 0.14 when super single tyres are replaced with dual tyres. From a different perspective, it also means that one pass of a 100 kN axle equipped with super single tyres causes greater damaging effect than 7 passes of 100 kN axles equipped with dual tyres. One pass of 100 kN axle with super single tyres also causes up to 2 times greater damage at the top of asphalt layers than an axle with the same load, but equipped with dual tyres.

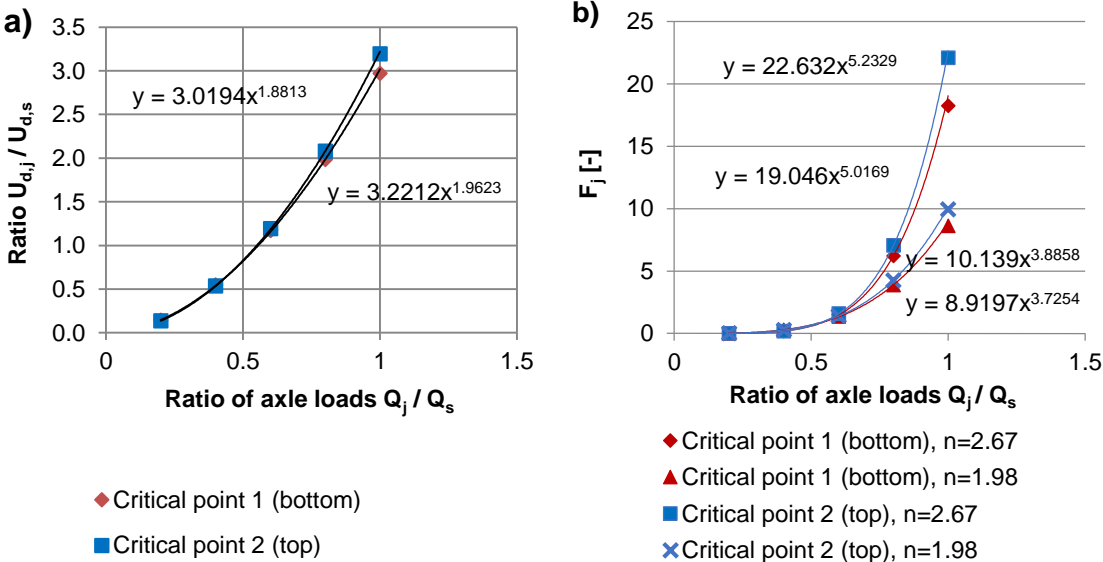***Equivalent axle load factors for triple axles with super single tyres***

According to the analysis delivered from Weigh-in-Motion (WIM) data collected by the Polish General Directorate for National Roads and Motorways, triple axles with single wheels represent around 20-25% of all axles of heavy vehicles (Rys et al., 2019). Similar statistic may be valid for highway and main road networks of most European countries (COST 334, 2001). This fact indicates that triple axles may greatly contribute to fatigue of asphalt pavements and correct evaluation of their effect is crucial for reliable prediction of the pavement service life. Model KR5 A1 was loaded by three single wheels moving at a distance of 1.3 m from each other in order to evaluate the effects of triple axles. The results of calculations related to strain energy of distortion $u_s$ for a triple axle are presented in Figure 6.

18
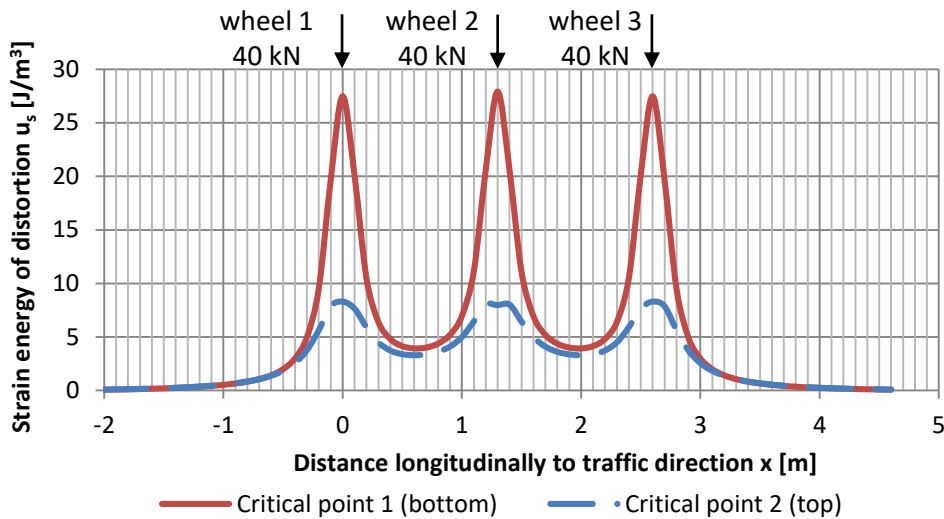
**Figure 6.** Strain energy of distortion $u_s$ induced by a triple axle with single wheels and the total load of 240 kN at critical points vs. the distance longitudinally to traffic direction,

On the basis of the results showed in Figure 6 it can be argued that more energy of distortion is induced in the bottom part of the pavement, similarly to the case of the pass of single axle (compare Figure 6 to Figure 2). Figure 7 presents relationships of the ratio $U_{d,j}/U_{d,s}$ and equivalent axle load factor $F_j$ for triple axles. It is noteworthy that a triple axle causes much greater damage to pavement structure than three single axles which carry the same load. Based on the comparison of power equations given in Figure 7b to power equations given in Figure 4b, the exponents $k$ (see equation (16)) are higher in the case of triple axle load. The effect of triple axles is also multiplied by the factor A, which ranges from 8.9 to 22.6, while for single axles A = 1. According to Figure 7 the equivalent axle load factor for a triple axle with total load Q = 240 kN (80 kN per each axle; therefore, for $Q_s$ = 100 kN the ratio $Q_j/Q_s$ = 0.8) is in the range from $F_j$ = 3.9 (critical point 1 at the bottom, $n$ = 1.98) to $F_j$ = 7.1 (critical point 2 on top, $n$ = 2.67). Three single axles with load of 80 kN each, but at a greater distance from each other, result in respective number of equivalent axle load passes: $3 \times 0.46$ = 1.38 (for critical point 1 at the bottom and $n$ = 1.98), and $3 \times 0.32$ = 0.96 (for critical point 2 on top and $n$ = 2.67). These values are calculated according to Figure 4 and the same ratio $Q_j/Q_s$ = 0.8.
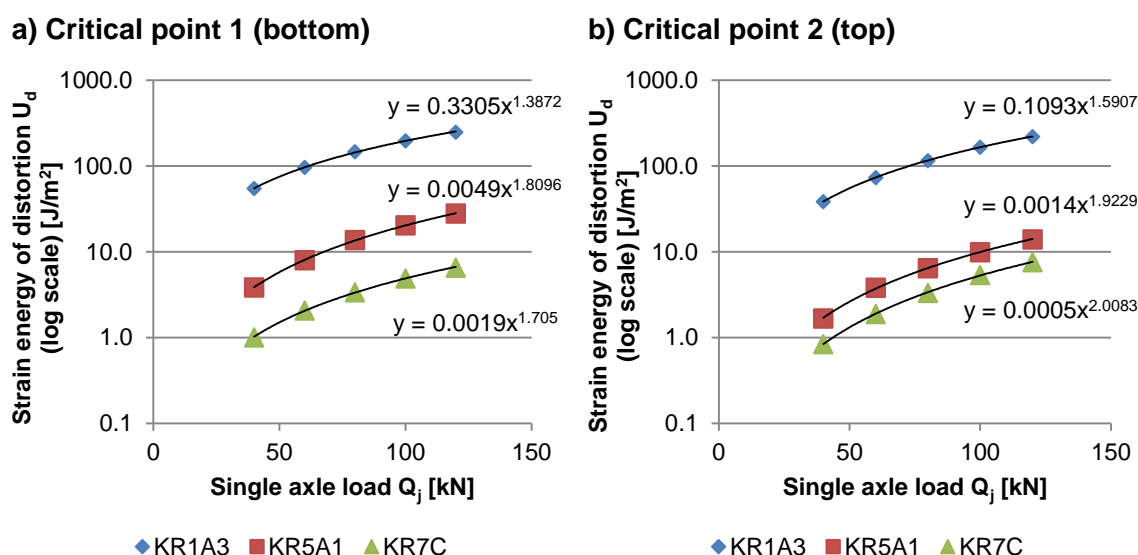
19

Therefore, the damaging effect of triple axles is increased by a factor of 2.9 (critical point 1 at the bottom, $n = 1.98$) to 7.4 (critical point 2 on top, $n = 2.67$) in comparison to three single axles with the same total load. This finding indicates that the effect of triple axles may be significantly underestimated in many pavement design methods.



**Figure 7.** a) Ratio between the total strain energy of distortion induced by actual triple axle vs. standard axle $U_{d,j}/U_{d,s}$ b) equivalent axle load factor $F_j$ for triple axle

### *Comparison of equivalent axle load factors for 3 types of pavement structures*

Equivalent standard axle load factors were calculated for three types of structures: KR1 A3, KR5 A1 and KR7 C. According to the presented method, at the first stage of the analysis the critical points with extreme values of strain energy of distortion $u_s$ were identified. The critical point at the bottom of asphalt layers is always located below the centre of the circular area of the single wheel load. In the case of thicker structures, KR5A1 and KR7 C, the critical point 2 (at the top of asphalt layers) appears near the edge of the circular load. The total strain energies of distortion $U_d$ were calculated and they are presented in relation to axle loads and critical point in Figure 8.

**a) Critical point 1 (bottom)**

$y = 0.3305x^{1.3872}$

$y = 0.0049x^{1.8096}$

$y = 0.0019x^{1.705}$

◆ KR1A3   ■ KR5A1   ▲ KR7C

**b) Critical point 2 (top)**

$y = 0.1093x^{1.5907}$

$y = 0.0014x^{1.9229}$

$y = 0.0005x^{2.0083}$

◆ KR1A3   ■ KR5A1   ▲ KR7C

**Figure 8.** Comparison of the total strain energy of distortion introduced by a pass of single axle in a) critical point 1 (at the bottom) and b) critical point 2 (at the top)

According to Figure 8, strain energy of distortion under the same axle load is lower for stronger structures and the value is around 100 times greater for the considered thin structure KR1A3 than for the thick structure KR7C. It is worth underlining that for the semi-rigid structure KR7C values of strain energy of distortion $U_d$ calculated at the top of the asphalt layers are slightly higher than the values calculated at the bottom of the asphalt layers and, therefore, this type of pavement structure is more prone to failure caused by development of top-down cracking.

Exponents given in power equations presented in Figure 8 are higher in the case of critical point 2 (at the top of asphalt layers) and equal from 1.59 to 2.01. Exponents in the case of critical point 1 (at the bottom of asphalt layers) range from 1.39 to 1.81. The exponent $n$ in the power relationship is the same for relationships $Q_j$ vs. $U_d$ and $Q_j/Q_s$ vs. $U_d/U_{ds}$. When the exponents presented in equations given in Figure 8 are multiplied by the exponent $n$ (see equation (15)), which expresses the asphalt mixture fatigue properties, the obtained result gives the exponent $k$ in the well-known power equation (16). Figure 9 presents the calculated values

21

of $k$ for the considered three types of pavement structures, in relation to the critical point and to exponent $n$, which includes the asphalt mixture fatigue properties.
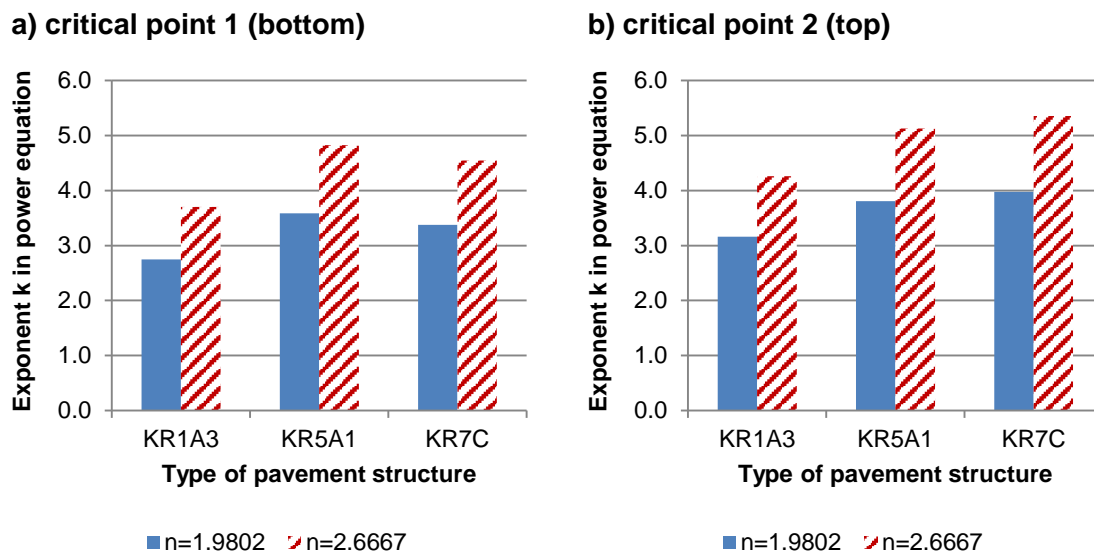


**Figure 9.** Comparison of the exponent $k$ in relation to the type of pavement structure

According to Figure 9, the exponent $k$ varies from 2.7 to 5.3. Asphalt mixture fatigue properties included in the exponent $n$ have a significant impact on the final value of the exponent $k$. A change of asphalt mixture fatigue properties from $n = 1.9802$ to $n = 2.6667$ results in an increase in the exponent $k$ by 35%. Exponent $k$ is lower for thinner flexible pavements than for thicker semi-rigid structures by around 17%. Location of the critical point has the lowest impact on the final exponent $k$. However, in the case of thick semi-rigid pavement KR7 C, the exponent $k$ is higher for the critical point 2 (at the top of asphalt layers) than for the critical point 1 (at the bottom of asphalt layers) by around 15%.

Calculations for triple axles as well as for single axle equipped with dual tyres were performed for each of the considered structures. The results of those calculations are summarized in Table 3 as exponent $k$ and factor $A$ according to Equation (16). Results in Table 3 are presented as ranges (minimum to maximum value), depending on the location of the critical point as well as the value of exponent $n$ related to the fatigue properties of asphalt mixture.

**Table 3.** Summary of coefficient $A$ and exponent $k$ in power equation for three considered pavement structures

| Pavement structure | Single axle | | | | | Triple axles with super single wheels | | | |
|---|---|---|---|---|---|---|---|---|---|
| | Coefficient A for | | | | Exponent k | Coefficient A | | Exponent k | |
| | super single wheels | dual tyre wheels | | | | | | | |
| | | min | max | min | max | min | max | min | max |
| KR1A3 | 1.0 | 0.10 | 0.45 | 2.7 | 4.3 | 6.8 | 16.1 | 3.1 | 4.7 |
| KR5A1 | 1.0 | 0.14 | 0.59 | 3.6 | 5.1 | 8.9 | 22.6 | 3.7 | 5.2 |
| KR7C | 1.0 | 0.09 | 0.47 | 3.4 | 5.4 | 8.2 | 27.5 | 3.6 | 5.3 |

According to Table 3, it can be concluded that triple axles are more aggressive for thicker structures, as demonstrated by the increase in coefficient A and exponent $k$. The value of EALF of axles equipped with dual tyres ranges from 0.09 to 0.59 of the corresponding value of EALF of axle with the same load, but equipped with super single tyres. Higher damaging effect of super single tyres in comparison to dual tyres is comparable across all structures and no evident trend is observed.

**Comparison of the new method with existing methods**

The new method was compared with previously developed methods including fourth power equation, *AASHTO Guide for Pavement Design (*1993), *French Design Manual for Pavement Structures, Guide technique* (1997) and COST 334 (2001). Truck factors (see equations (10)-(12)) were calculated for each method and compared. For this purpose, an example of axle load spectra (ALS) related to a heavy vehicle composed of 2-axle tractor with a semitrailer equipped with triple axle were assumed, as presented in Figure 10. This choice is based on recent traffic analyses of multilane main roads, which have shown that this type of truck represents up to 80% of the total number of heavy vehicles. As a consequence, any possible errors in evaluation

of pavement damage induced by the tractor-semitrailer vehicle may lead to significant misprediction of the total pavement service life.

The ALS were obtained on the basis of data from Polish weigh-in-motion station located on the motorway A2 near the city of Lodz. More details about the source of weigh-in-motion data and methodology of its analysis used by the authors are given in previous publications (Rys, 2019; Rys & Burnos, 2021).
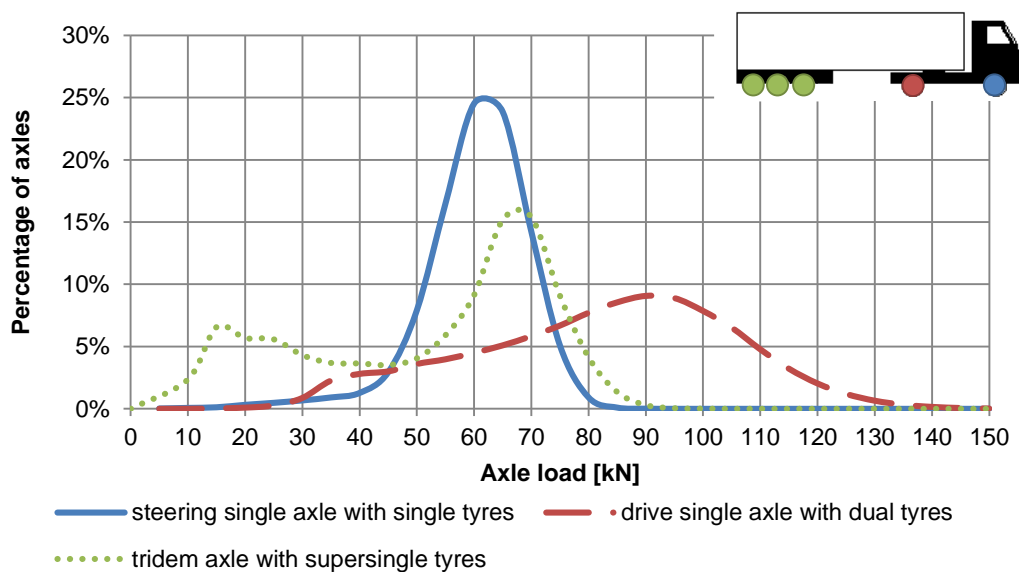


**Figure 10.** Axle load spectra used for calculations of truck factors

Fourth power equation does not include the effect of triple axles nor the differentiation between single vs. dual tyres. In the AAHTO 1993 equations, the effect of multiple axles is included. Calculations according to AASHTO 1993 were performed with assumption of the structural number SN = 5.15 and terminal serviceability index $p_t$ = 2.5. In the method developed in COST 334, the effect of super single tyres and dual tyres is included, and for the purpose of this analysis the super single tyre 425/65R22.5 was assumed as the standard wheel. The method also assumed the power exponent equal to 2 in the power equation (16). In the French design method, the power equation (16) includes exponent equal to 5 and the effect of multiple axles is included in the coefficient A = 1.1. Comparison of truck factors calculated for different methods is presented in Figure 11. In Figure 11 the minimum and maximum truck factors

according to the new method represent critical point 1 (at the bottom) and material coefficient $n = 1.98$ and critical point 2 (on top) and material coefficient $n = 2.67$, respectively.
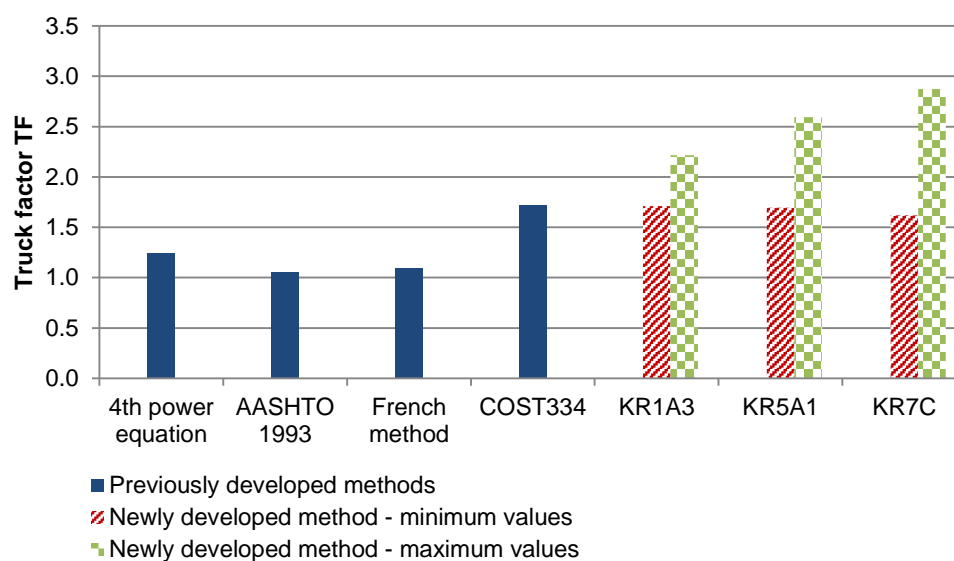


**Figure 11.** Comparison of truck factors calculated according to the newly developed method and truck factors calculated with selected existing methods

On the basis of Figure 11 it can be concluded that minimum values of truck factors calculated according to the presented new method are close to those obtained with the method proposed in COST 334. The new method delivered truck factors 1.8 to 3.3 times higher than the 4th power equation, AASHTO 1993 and French method. It results from the fact that the damaging effect of triple axles according to the new method is much higher than in other methods. Higher truck factor in combination with higher strain energy of distortion at the top of asphalt layers can be one of possible reasons of top-down cracks observed on thick and stiff pavements.

**Conclusions**

1) The new method of calculation of equivalent axle load factor was developed and described in the paper. The method is based on the analysis of strain energy of distortion introduced into the pavement by a pass of a vehicle wheel. When single axles are

25

considered, the new method delivers similar results as the well-known power equation, and the power exponent ranges from 2.7 to 5.3.

2) It was noted that strain energy of distortion reaches extreme values in two critical points: at the bottom and at the top of asphalt layers. In the case of heavy axle loads and thick structures, strain energy of distortion at the top of asphalt layers reaches higher values than at the bottom of asphalt layers. The ratio between the values of the total strain energy of distortion introduced by the actual axle vs. the standard axle $U_{d,j}$ / $U_{d,s}$ is strongly related with the ratio between the actual axle load and standard axle load $Q_j/Q_s$ and the power exponent in those relationships equals approximately 2.

3) Fatigue properties of asphalt mixtures are included in the exponent $k$ of power equation and they have a significant impact on the calculated equivalent axle load factor. A change in fatigue properties of the asphalt mixture may result in differences in the final value of the exponent $k$ reaching 35%. The type and thickness of the asphalt pavement also has impact on the exponent $k$ in power equation. The exponent $k$ and is lower by around 17% for the thin flexible pavement labelled KR1A3 than for the thick semi-rigid pavement labelled KR7C.

4) The main advantage of the new method consists in a more accurate calculation of equivalent axle load factor for multiple axles. The method also enables distinguishing the effects of super single and dual tyres. Analysis proved that the damaging effect of triple axles is 2.9 to 7.4 times greater than the damaging effect of three single axles carrying the same load. According to calculations, replacement of a super single tyre by a dual tyre results in reduction of equivalent axle load factor by a coefficient ranging from 0.1 to 0.6.

5) The newly developed method was compared with existing methods used for calculation of the number of equivalent standard axle loads for pavement design. For this purpose, truck factors were calculated for a sample axle load spectrum obtained from weighing of vehicles in motion. The new method delivered truck factors 1.8 to 3.3 times greater than the $4^{th}$ power equation, AASHTO 1993 and French method. They were close to factors obtained according to COST 334. The source of the observed difference is the fact that load equivalency factors obtained for triple axles according to the new method are several times greater. The effect of triple axles may be significantly underestimated in many pavement design methods, resulting in erroneously reduced values of truck factors assumed for pavement design and, consequently, in overestimation of the pavement service life. The latter occurs very often, likely due to adoption of wrong models for the calculation of equivalent axle load factors, leading to detrimental effects in terms of pavement management strategies and the need for premature repair and rehabilitation works.

**Acknowledgement**

**References**

*AASHTO Guide for Pavement Design 1993*. (1993). Washington D.C., USA: American Association of State and Highway Transportation Officials.

ARA Inc. (2004). *Guide for Mechanistic-Empirical Design of New and Rehabilitated Pavement Structures. Part 3. Chapter 3. Design of New and Reconstructed Flexible Pavements.* Washington: Transportation Research Board. Retrieved from

www.trb.org/mepdg

Atkinson, V. M., Merrill, D., & Thom, N. (2005). *Pavement wear factors, TRL Published Project Report PPR 066.*

Beer, D., Fisher, C., & Jooste, F. J. (1997). *Determination of Pneumatic Tyre-Pavement Interface Contact Stresses under Moving Loads and some Effects on Pavements with Thin Asphalt Surfacing Layers*. *8th International Conference on Asphalt Pavements* (Vol. 1).

Bhasin, A., Castelo Branco, V. T., Masad, E., & Little, D. N. (2009). Quantitative Comparison of Energy Methods to Characterize Fatigue in Asphalt Materials. *Journal of Materials in Civil Engineering*, *21*(2), 83–92. https://doi.org/10.1061/(asce)0899-1561(2009)21:2(83)

Braham, A., & Underwood, B. S. (2016). State of the Art and Practice in Fatigue Cracking Evaluation of Asphalt Concrete Pavements. *Association of Asphalt Paving Technologists*, 156. Retrieved from http://asphalttechnology.org/downloads/Fatigue_Cracking_of_Asphalt_Pavements_2017 _06.pdf

Canestrari, F., & Ingrassia, L. P. (2020). A review of top-down cracking in asphalt pavements: Causes, models, experimental tools and future challenges. *Journal of Traffic and Transportation Engineering (English Edition)*, *7*(5), 541–572. https://doi.org/10.1016/j.jtte.2020.08.002

COST 334. (2001). Effects of wide single tyres and dual tyres: final report of the action, (version 29).

De Beer, M., Maina, J. W., Van Rensburg, Y., & Greben, J. M. (2012). Toward using tire-road contact stresses in pavement design and analysis. *Tire Science and Technology*, *40*(4), 246–271. https://doi.org/10.2346/tire.12.400403

*French Design Manual for Pavement Structures, Guide technique*. (1997).

General Directorate for National Roads and Highways, (GDDKiA). (2014). *Catalog of Typical Flexible and Semi-Rigid Pavements*. Gdansk. Retrieved from https://www.gddkia.gov.pl/userfiles/articles/z/zarzadzenia-generalnego-dyrektor_13901/zarzadzenie 31 zalacznik.pdf

Ghuzlan, K. A., & Carpenter, S. H. (2000). Energy-derived, damage-based failure criterion for fatigue testing. *Transportation Research Record*, (1723), 141–149. https://doi.org/10.3141/1723-18

Hamlat, S., Hammoum, F., & Kerzreho, J. P. (2015). Evaluation of the distribution of local pressures and the real contact area between the tyre and the road surface. *International Journal of Pavement Engineering*, *16*(9), 832–841. https://doi.org/10.1080/10298436.2014.961021

Hernandez, J. A., Gamez, A., Al-Qadi, I. L., & De Beer, M. (2014). Analytical approach for predicting three-dimensional tire-pavement contact load. *Transportation Research Record*, *2456*, 75–84. https://doi.org/10.3141/2456-08

Huber, M. T. (1904). Specific work of strain as a measure of material effort (a Translation from the original paper from Polish by Anna Stręk under scientific supervision of Ryszard B. Pęcherski). *Archives of Mechanics*, *56*(3), 173–190.

Judycki, J., Jaskuła, P., Pszczoła, M., Ryś, D., Jaczewski, M., Alenowicz, J., … Stienss, M. (2017). New polish catalogue of typical flexible and semi-rigid pavements. In *MATEC Web of Conferences* (Vol. 122). https://doi.org/10.1051/matecconf/201712204002

Judycki, Jozef. (2010). Determination of Equivalent Axle Load Factors on the Basis of Fatigue Criteria for Flexible and Semi-Rigid Pavements. *Road Materials and Pavement Design*, *11*(1), 187–202. https://doi.org/10.1080/14680629.2010.9690266

Judycki, Jozef. (2011). Equivalent Axle Load Factors for Design of Rigid Pavements Derived

from Fatigue Criteria. *The Baltic Journal of Road and Bridge Engineering*, *6*(4), 219–224. https://doi.org/10.3846/bjrbe.2011.28

Mackiewicz, P. (2018). Fatigue cracking in road pavement. *IOP Conference Series: Materials Science and Engineering*, *356*(1). https://doi.org/10.1088/1757-899X/356/1/012014

Moreno-Navarro, F., & Rubio-Gámez, M. C. (2016). A review of fatigue damage in bituminous mixtures: Understanding the phenomenon from a new perspective. *Construction and Building Materials*, *113*, 927–938. https://doi.org/10.1016/j.conbuildmat.2016.03.126

Perdomo, D., & Nokes, B. (1993). Theoretical analysis of the effects of wide-base tires on flexible pavements using CIRCLY. *Transportation Research Record*, (1388), 108–119.

Rys, D. (2019). Investigation of weigh-in-motion measurement accuracy on the basis of steering axle load spectra. *Sensors (Switzerland)*, *19*(15). https://doi.org/10.3390/s19153272

Rys, D., Judycki, J., & Jaskula, P. (2016). Determination of Vehicles Load Equivalency Factors for Polish Catalogue of Typical Flexible and Semi-rigid Pavement Structures. In *Transportation Research Procedia* (Vol. 14). https://doi.org/10.1016/j.trpro.2016.05.272

Rys, Dawid, & Burnos, P. (2021). Study on the accuracy of axle load spectra used for pavement design. *International Journal of Pavement Engineering*, *0*(0), 1–10. https://doi.org/10.1080/10298436.2021.1915492

Sabouri, M., & Kim, Y. R. (2014). Development of a failure criterion for asphalt mixtures under different modes of fatigue loading. *Transportation Research Record*, *2447*(December 2014), 117–125. https://doi.org/10.3141/2447-13

Shen, S., Airey, G. D., Carpenter, S. H., & Huang, H. (2006). A Dissipated Energy Approach to Fatigue Evaluation. *Road Materials and Pavement Design*, *7*(1), 47–69. https://doi.org/10.1080/14680629.2006.9690026

30

Shen, S., & Carpenter, S. H. (2007). Development of an asphalt fatigue model based on energy principles. *Asphalt Paving Technology: Association of Asphalt Paving Technologists-Proceedings of the Technical Sessions*, *76*(October), 525–573.

Sieber, R. (2012). *Guidelines for design of the pavement structures of traffic areas RSTO 12*. Leipzig, Germany.

van Dijk, W. (1975). V44-P038.Pdf. *American Association of Asphalt Pavement Technologiests*, *44*, 38–74.

van Dijk, W., & Visser, W. (1977). The energy approach to fatigue for pavement desig. *AAPT Annual Meeting*, *46*, 1–40.

von Mises, R. (1913). Mechanik der festen Körper im plastisch- deformablen Zustand. *Achrichten von Der Gesellschaft Der Wissenschaften Zu Göttingen, Mathematisch-Physikalische Klasse*, *4*, 582–592. Retrieved from http://www.digizeitschriften.de/dms/img/?PID=GDZPPN002503697

Zhang, J., Sabouri, M., Guddati, M. N., & Kim, Y. R. (2013). Development of a failure criterion for asphalt mixtures under fatigue loading. *Road Materials and Pavement Design*, *14*(June 2014), 1–15. https://doi.org/10.1080/14680629.2013.812843